基于布洛克磁共振流动方程和贝塞尔函数的磁共振成像序列数学设计

O.B. Awojoyogbe*, O.M. Dada

作者单位：
尼日利亚联邦科技大学物理系

通讯作者：
O.B. Awojoyogbe，
E-mail：awojoyogbe@yahoo.com

收稿日期：2013-03-06
接受日期：2013-07-18

中图分类号：R445.2
文献标识码：A
DOI: 10.3969/j.issn.1674-8034.2013.05.011

Awojoyogbe OB, Dada OM. 基于布洛克磁共振流动方程和贝塞尔函数的磁共振成像序列数学设计. 磁共振成像, 2013, 5(1): 373-381.

[摘要] Bloch方程是NMR/MRI计算、模拟和实验的基础，但通常在不加特定的绝热和非绝热条件的前提下获得Bloch流动方程的解析解是非常困难的。流动方程的一般解析解可以为理解NMR/MRI的基本概念提供额外的信息，而又不需要通常的指数方程。作者的目的是通过贝塞尔函数及其特性得到与时间无关的NMR流动方程的解析解。在不需要主观添加弥散项的前提下利用贝塞尔函数及其特性从NMR流动方程中获得了Stejskal-Tanner公式。这证实了弥散是Bloch流动方程的内在属性并可以通过如贝塞尔函数的适当数学函数提取出来。从解析解得到的非高斯行为的弥散信号在如脑白质的各项异性组织环境中是非常有意义的。发现弥散系数是与 T1 和T2弛豫参数直接相关的，因此通过对大量已有的贝塞尔函数进行合适利用可以在四个分离的缓存内采集MRI信号(实部和虚部，相位和绝对值)。能够利用MRI监测药物对于不同组织尤其是脑部功能活动的效果。

[关键词] 弥散磁共振成像；Bloch磁共振方程；贝塞尔函数；曲折度和各向异性的组织环境

Mathematical design of a magnetic resonance imaging sequence based on bloch NMR flow equations and bessel functions

O.B. Awojoyogbe*, O.M. Dada
Department of Physics, Federal University of Technology, Minna, Niger-State, Nigeria
*Correspondence to: Awojoyogbe OB, E-mail: awojoyogbe@yahoo.com
Received 6 Mar 2013, Accepted 18 July 2013

Abstract Bloch NMR equations are fundamental to all NMR/MRI computations, simulations and experiments. It has been very difficult to solve the Bloch NMR flow equations analytically without imposing specific adiabatic and non adiabatic conditions. General analytical solutions of the flow equations can easily provide additional information to understand the basic concept of NMR/MRI without the usual exponential functions. The goal of this report is to present analytical solutions to the time independent NMR flow equation using the Bessel functions and properties. We derived the Stejskal-Tanner formula from the NMR flow equations using the Bessel functions and properties without the need to arbitrarily add the diffusion term. This confirms that diffusion is an intrinsic property embedded in the Bloch NMR flow equation and can be extracted by the use of appropriate mathematical functions such as Bessel functions and properties. The analytical solutions result in a non-Gaussian behavior of the diffusion signal which may be very useful when tissue environment is anisotropic such as in white matter of the brain. It is exciting to note that the diffusion coefficient is directly related to the T_1 and T_2 relaxation parameters. The abundantly available Bessel functions and properties can then be appropriately applied to acquire MRI signals in four separate buffers (real and imaginary parts as well as phase and absolute value). We may be able to monitor the effects of drugs on the functional activities of different tissues especially the brain by means of magnetic resonance Imaging.

Key words Diffusion magnetic resonance imaging; Bloch NMR equations; Bessel functions; Tortuosity and anisotropic tissue environment

1 Introduction

The tortuosity parameter[1-8] describes geometrical hindrance of an environment relative to an obstacle-free medium. If the obstacles exhibit some directional preference, the hindrance becomes anisotropic, that is, it depends on direction. For example, the molecules diffuse more readily along the white matter fibers than across them. In a macroscopically homogeneous and anisotropic environment, the tortuosity takes the shape of a symmetric tensor of the second order, which can be represented by a 3×3 matrix with six independent values. The tortuosity tensor combines with the scalar free diffusion coefficient into a tensor of apparent diffusion $\vec{D}$. However, despite all these complexities, the pulse field gradient method proposed by Stejskal and Tanner is still used to calculate signal attenuation due to diffusion along any single direction of the diffusion gradient. The only real difference from the homogeneous and isotropic case is that the experiment must be repeated using at least six non-collinear directions of the diffusion gradient to obtain six independent components of the apparent diffusion tensor. It is therefore fair to conclude that the pulse field gradient method proposed by Stejskal and Tanner is at the heart of most modern diffusion and DTI experiments.

DTI has become a very popular MR imaging modality and is developing into an important tool for non-invasive study and characterization of the brain white matter. It has been applied to the study of many neurological brain disorders such as schizophrenia, cocaine addiction, HIV infection, alcoholism, geriatric depression and Alzheimer's disease. An overview of theoretical issues surrounding the DTI technique can be found in literature[9-11]. A review of DTI applications in neuroscience is presented by Lim and Helpern[12].

It is our view that good understanding of the Stejskal-Tanner formulae is essential for logical design or interpretation of any MR diffusion experiment. Unfortunately, the derivation in a completely general case is nontrivial as it involves solving the Bloch-Torrey partial differential equations[4-5]. We need to briefly review a simple connection between Gaussian diffusion and random walks. A comprehensive treatment can be found, for example, in works of Callagan, Haacke et al and Chandrasekhar[13-15].

If we begin with a qualitative description (within the rotating frame of reference) of diffusion on the NMR signal, an RF pulse turns all the equilibrium magnetization M_0 into the transverse plane, perpendicular to the main static magnetic field B_0. The magnetization vector will rotate around it at angular frequency $\omega = \frac{d\varphi}{dt}$ given by the Larmor equation: $\omega = \gamma B_0$.

Where γ is the gyromagnetic ratio (for a hydrogen proton). After the excitation, a short and strong gradient G is applied along the x-axis, changing the constant main field B_0 to a spatially variable field

$$B(x) = B_0 + Gx = B_0 + B_1(x) \quad (1a)$$

Larmor frequencies therefore become different at different places along the x-axis. When the gradient is switched off again, some phase differences will have accumulated between the spins at different positions. At this point, we just wait for a period equal to the diffusion time $t=n\Delta t$. Then an opposite but otherwise identical gradient, $-G$, is applied. If the atoms did not change their positions during the diffusion time, all the phase differences would be perfectly reversed and the magnetization would be fully restored (apart from the neglected relaxation effects). However, if the spins move, the second gradient finds them at different locations than the first one and the phases will be reversed "incorrectly". The result is phase dispersion in the measured sample and loss of signal when all the spins are eventually summed up to form the magnetization vector. Faster diffusion (larger D) means that the spins have bigger chance to travel farther and therefore experience larger magnetic field changes due to diffusion gradients. This causes larger spread in the phases and therefore results in a smaller signal.

Bloch NMR flow equations, describing the

dynamics of the magnetization vector, have been solved analytically by imposing specific adiabatic and non adiabatic conditions[16- 22]:

$$\gamma^2 B_1^2(x) >> \frac{1}{T_1 T_2} \quad (1b)$$

$$\gamma^2 B_1^2(x) << \frac{1}{T_1 T_2} \quad (1c)$$

It may be very important to solve the flow equation for general cases without imposing these conditions.

In this investigation, we solved the NMR flow equation for general cases using the Bessel properties and functions as mathematical tools to obtain the NMR transverse magnetization and the diffusion coefficient which depends on NMR relaxation parameters. The NMR system is considered in both real and complex domains which can easily provide additional information to understand the basic concept of NMR/MRI without the usual exponential functions.

2 Mathematical formulation

Specifically, we consider the fluid particle (on the atomic scale) which either initially or in some average sense is in steady rotation. We apply a mathematical algorithm to describe in detail the dynamical state of the flowing fluid particle starting from the Bloch NMR flow equations[18-20]. We study the flow properties of the modified time independent Bloch NMR flow equations which describe the dynamics of fluid flow under the influence of RF magnetic field as derived in the earlier studies[16-22] when resonance condition exists at Larmor frequency:

$$f_o = \gamma B - \omega = 0 \quad (1d)$$

Then the *x, y, z* components (in the rotating frame) of the magnetization of a fluid bolus moving with variable velocity $v(x)$ is given by the Bloch equations which may be written as follows:

$$\frac{dM_x}{dt} = v(x) grad M_x + \frac{\partial M_x}{\partial t} = -\frac{M_x}{T_2} \quad (1e)$$

$$\frac{dM_y}{dt} = v(x) grad M_y + \frac{\partial M_y}{\partial t} = \gamma M_z B_1(x) - \frac{M_y}{T_2} \quad (1f)$$

$$\frac{dM_z}{dt} = v(x) grad M_z + \frac{\partial M_z}{\partial t} = -\gamma M_y B_1(x) + \frac{(M_0 - M_z)}{T_1} \quad (1g)$$

Subject to the following conditions:

i. $M_o \neq M_z$ a situation which holds well in general and in particular when the RF$B_1(x)$ field is strong say of the order of 1.0G or more.

ii. Before entering signal detector coil, fluid particles has magnetization $M_x = 0$, $M_y = 0$.

iii. If $B_1(x)$ is large, $B_1(x) >> 1$G or more so that M_y of the fluid bolus changes appreciably from M_o.

iv. In anisotropic diffusion, the diffusion coefficient, D = D(x), $v(x) = u_0 x$ and $u_0 = \frac{1}{\delta}$ where t is considered a constant.

γ denotes the gyromagnetic ratio of fluid spins, $\omega/2\pi$ is the RF excitation frequency, f_0/γ is the off-resonance field in the rot ating frame of reference.T_1 and T_2 are the spin-lattice and spin-spin relaxation times respectively, the reciprocals of T_1 and T_2 are defined as relaxation rates. RF B_1 is the spatially varying magnetic field and v is the fluid flow velocity. Equations (1f and 1g) give a second order non – homogeneous differential equation which may be fundamental for the development of new magnetic resonance techniques. Hence, the Bloch NMR flow equation becomes:

$$v^2 \frac{d^2 M_y}{dx^2} + v\left(\frac{1}{T_1} + \frac{1}{T_2}\right)\frac{dM_y}{dx} + \left(\gamma^2 B_1^2(x) + \frac{1}{T_1 T_2}\right) M_y = \frac{M_o \gamma B_1(x)}{T_1} \quad (2a)$$

Subject to the following definition:

(i) for steady flow, $\frac{\partial M_y}{\partial t} = 0$ (2b)

(ii) $v(x) = \frac{x}{\delta}$ (3a)

Therefore, we may write:

$$\gamma B_1(x) = \alpha x^q \quad (3b)$$

where q is an integer and

$$\alpha = \gamma G \quad (3c)$$

In a typical MRI procedure, *G* is the pulsed gradient applied for the length of time δ and *q*=1. However, for spin magnetization which is independent of the length of time *t* (constant time), we shall substitute for equations (1a) and (3) in equation (2) :

$$x^2 \frac{d^2 M_y}{dx^2} + \delta x\left(1 + \frac{1}{T_1} + \frac{1}{T_2}\right)\frac{dM_y}{dx} + \left((\gamma \delta G)^2 x^2 + \frac{\delta^2}{T_1 T_2}\right) M_y = \frac{M_o \gamma B_1(x)}{T_1} \quad (4)$$

Tab. 1 Values of the relaxation times[23] of human tissues at 1.5 T as they relate to the Bessel function parameters

Tissues	T_1(s)	T_2(s)	t(s)	T_1T_2(s^2)	T_0(s^{-1})	k	β^2	m_0
Skeletal muscle	1.03	0.06	2.0	0.0618	17.63754	18.13754	64.72492	16.25563
Heart muscle	1.01	0.073	2.0	0.07373	14.68873	15.18873	54.252	13.28328
Liver	0.61	0.057	2.0	0.03477	19.1832	19.6832	115.0417	16.50415
Kidney	0.83	0.082	2.0	0.06806	13.39994	13.89994	58.77167	11.59468
Spleen	0.93	0.089	2.0	0.08277	12.31122	12.81122	48.32669	10.76108
Fatty tissue	0.33	0.12	2.0	0.0396	11.36364	11.86364	101.0101	6.303631
Gray brain matter	1.08	0.124	2.0	0.13392	8.990442	9.490442	29.86858	7.75886
White brain matter	0.92	0.114	2.0	0.10488	9.858886	10.35889	38.13883	8.316712

When the radiofrequency field turns all the equilibrium magnetization M_0 into the transverse plane, perpendicular to the main static magnetic field B_0, maximum signal is expected for maximum RF $B_1(x)$ field and M_0 is minimum (say $M_0 \approx 0$). For a maximum value of M_y, we can write equation (4) as follows:

$$x^2\frac{d^2M_y}{dx^2}+\delta\left(1+\frac{1}{T_1}+\frac{1}{T_2}\right)x\frac{dM_y}{dx}+\left(\lambda^2x^2+\beta^2\right)M_y=0 \tag{5}$$

Equation (5) is a general form of an equation transformable into Bessel's equation of order β with parameter λ. A general solution of equation (5) is in the form:

$$M_y(x)=x^{-k}\left[c_1J_{\frac{m_0}{\eta}}\left(\frac{\lambda x^\eta}{\eta}\right)+c_2Y_{\frac{m_0}{\eta}}\left(\frac{\lambda x^\eta}{\eta}\right)\right] \tag{6}$$

where k, m_0, η, β are all constants defined as:

$$m_0=\sqrt{k^2-\beta^2} \tag{7}$$

$$\lambda=\gamma\delta G \tag{8}$$

$$\beta^2=\frac{\delta^2}{T_1T_2} \tag{9}$$

$$k=\frac{\delta(1+T_o)-1}{2} \tag{10}$$

$$T_0=\left(\frac{1}{T_1}+\frac{1}{T_2}\right)=\frac{(T_1+T_2)}{T_1T_2} \text{ and } \eta=1$$

Equation (6) therefore becomes:

$$M_y(x)=x^{-k}\left[c_1J_{m_0}(\lambda x)+c_2Y_{m_0}(\lambda x)\right] \tag{11}$$

Since the transverse magnetization needs to have a finite limit as x tends to zero, c_2=0 and if we set the constant, c_1=1, we have:

$$M_y=x^{-k}J_{m_0}(\lambda x) \tag{12}$$

3 Complex radio frequency magnetic field

In equation (3a), if the applied radio frequency field when k = 0 and q=1 is complex for a complex system, we may write:

$$\gamma B_1(x)=i\alpha x \tag{13}$$

It should be noted that in the light of equations (6) and (7), we may write $m_0^2=-m^2=-\beta^2=-\frac{\delta^2}{T_1T_2}$. Therefore, we can write equations (11) as

$$M_y(x)=\left[c_1I_m(\lambda x)+c_2K_m(\lambda x)\right] \tag{14}$$

In this case, β is not restricted. If β is not an integer, we have the alternative form

$$M_y(x)=\left[c_1I_m(\lambda x)+c_2I_{-m}(\lambda x)\right] \tag{15}$$

It may be useful especially in diffusion MRI to consider the applied radio frequency field in equation (3b) as complex function when k = 0 and q=1 given as follows:

$$\gamma B(x)=\sqrt{-i}\alpha x \tag{16}$$

We can write the NMR transverse magnetization as

$$M_y(x)=c_1(ber_m\lambda x+ibei_m\lambda x)+c_2(\ker_m\lambda x+ikei_m\lambda x) \tag{17}$$

In equation (17), for real values of x the equation

$$F_m(x)=\sqrt{ber_m^2\lambda x+ibei_m^2\lambda x} \tag{18}$$

Is a complex number with characteristic length or modulus $F_m(x)$ and a characteristic angle or amplitude

$$A_m(x)=\tan^{-1}\frac{bei_m(\lambda x)}{ber_m(\lambda x)} \tag{19}$$

It may be more useful to replace the expression $ber_m(x)+ibei_m(x)$ by the exponential expression $F_m(x)e^{iA_m(x)}$. Similarly, the equation

$$H_m(x)=\sqrt{\ker_m^2(\lambda x)+ikei_m^2(\lambda x)} \quad (20)$$

has a characteristic length or modulus, $H_m(x)$ and a characteristic angle of amplitude

$$B_m(x)=\tan^{-1}\frac{kei_m(\lambda x)}{\ker_m(\lambda x)} \quad (21)$$

The expression $\ker_m x+i\, kei_m x$ can also be replaced by the exponential expression $H_m(x)e^{iB_m(x)}$.

We can finally write equation (17) as

$$M_y(x)=\left[c_1F_m(x)e^{iA_m(x)}+c_2H_m(x)e^{iB_m(x)}\right] \quad (22)$$

The Bessel functions and properties when k =0 in equation (9) are readily available for the analysis of MRI signals as derived in equations (12, 14, 15, 17,22) , These functions have been graphically displayed for certain important values of relaxation parameter m when λ is a unit parameter either real of complex[24-27]. The measurement may be carried out by varying either the magnitude G, of the pulsed gradient or the length of time $\tau=\delta$, the time between pulses in the experiment. This sum is best tackled using the Euler theorem exp $iA(x)$=cos$A(x)$ + i sin$A(x)$.

Abbreviating the expression, we have:

$$A(x)=-\gamma G\Delta x\delta \quad (23a)$$

Therefore, we derive[13-15]

$$S=M_0\cos^n(A)=M_0\cos^n(\gamma G\delta\Delta x)$$

The NMR signal undergoes various stages of amplification, filtering and other transformations. It is therefore not possible to measure M_0 in absolute terms. We can remedy this unfortunate drawback of NMR by measuring the same sample twice: once without the diffusion gradients, to obtain un-attenuated signal S_0, and once with them, to obtain signal S. The M_0 term in the signal will stay the same but the attenuation term will disappear from S_0. We then calculate the ratio of the signals with and without the diffusion gradients:

$$\frac{S}{S_0}=\frac{M_0\cos^n(\gamma G\delta\Delta x)}{M_0}=\cos^n(\gamma G\delta\Delta x)$$

The last step is to eliminate Δx and express the result in terms of experimentally accessible variables.

$$\gamma G\delta\Delta x=\sqrt{\gamma^2G^2\delta^2\Delta x^2}=\sqrt{2\left(\gamma^2G^2\delta^2n\Delta t\right)\frac{1}{n}\frac{\Delta x^2}{2\Delta t}}=\sqrt{\left(\gamma^2G^2\delta^2\tau\right)\frac{D}{n}}=\sqrt{\frac{2bD}{n}} \quad (23b)$$

where the so-called b –value is introduced[13-15],

$$b=\gamma^2G^2\delta^2\tau \quad (24)$$

S is the signal strength in a pulse sequence with a pair of balanced diffusion-sensitizing gradients of strength G, each of a duration δ and with a delay τ between them. S_0 is the signal strength in an identical experiment but without the diffusion gradient pair. When it can be safely assumed that $\delta<<\tau$, the expression for b (usually called b-value) simplifies to equation (24). Equation (22) becomes

$$M_y(x)=\left[c_1F_m(x)e^{-bD_{1m}}+c_2H_m(x)e^{-bD_{2m}}\right] \quad (25)$$

where D_{1m} and D_{2m} may represent diffusion coefficients in different locations in the voxel of anisotropic tissue. These diffusion coefficients can be analyzed using the Bessel properties in equations (19, 21) as:

$$D_{1m}=-\frac{1}{b}\tan^{-1}\frac{bei_m(\lambda x)}{ber_m(\lambda x)}=-\frac{1}{b}\tan^{-1}\left\{\frac{\sum_{f=0}^{\infty}\frac{\left[\sin(3m/4+f/2)\pi\right]}{2^{m+2f}\,f!\Gamma(m+f+1)}(\lambda x)^{m+2f}}{\sum_{f=0}^{\infty}\frac{\left[\cos(3m/4+f/2)\pi\right]}{2^{m+2f}\,f!\Gamma(m+f+1)}(\lambda x)^{m+2f}}\right\} \quad (26a)$$

$$D_{2m}=-\frac{1}{b}\tan^{-1}\frac{kei_m(\lambda x)}{\ker_m(\lambda x)} \quad (26b)$$

If we set m=1/2 in equation (26a), we have the following expressions:

$$D_{1/2}=-\frac{1}{b}\tan^{-1}\frac{bei_{1/2}(\lambda x\sqrt{2})}{ber_{1/2}(\lambda x\sqrt{2})}=-\frac{1}{b}\tan^{-1}\left\{\frac{\frac{2^{-3/4}}{\sqrt{\pi\lambda x}}\left(e^{\lambda x}\sin(\lambda x+\frac{\pi}{8})+e^{-\lambda x}\sin(\lambda x-\frac{\pi}{8})\right)}{\frac{2^{-3/4}}{\sqrt{\pi\lambda x}}\left(e^{\lambda x}\cos(\lambda x+\frac{\pi}{8})-e^{-\lambda x}\cos(\lambda x-\frac{\pi}{8})\right)}\right\} \quad (27a)$$

$$D_{1/2}-\frac{1}{b}\tan^{-1}\left\{\frac{\left(e^{\lambda x}\sin(\lambda x+\frac{\pi}{8})+e^{-\lambda x}\sin(\lambda x-\frac{\pi}{8})\right)}{\left(e^{\lambda x}\cos(\lambda x+\frac{\pi}{8})-e^{-\lambda x}\cos(\lambda x-\frac{\pi}{8})\right)}\right\} \quad (27b)$$

Tab. 2 Values of the relaxation times of human tissues at 1.5 T [23] as they relate to the Bessel parameters in the solutions (14), (15) and (22)

Tissues	T_1(s)	T_2(s)	δ (s)	$T_1T_2(s^2)$	$T_0(s^{-1})$	β^2	M
Skeletal muscle	1.03	0.06	1.0	0.0618	17.63754	16.18123	4.02259
Heart muscle	1.01	0.073	1.0	0.07373	14.68873	13.563	3.682798
Liver	0.61	0.057	1.0	0.03477	19.1832	28.76043	5.362875
Kidney	0.83	0.082	1.0	0.06806	13.39994	14.69292	3.833134
Spleen	0.93	0.089	1.0	0.08277	12.31122	12.08167	3.47587
Fatty tissue	0.33	0.12	1.0	0.0396	11.36364	25.25253	5.025189
Gray brain matter	1.08	0.124	1.0	0.13392	8.990442	7.467145	2.732608
White brain matter	0.92	0.114	1.0	0.10488	9.858886	9.534706	3.087832

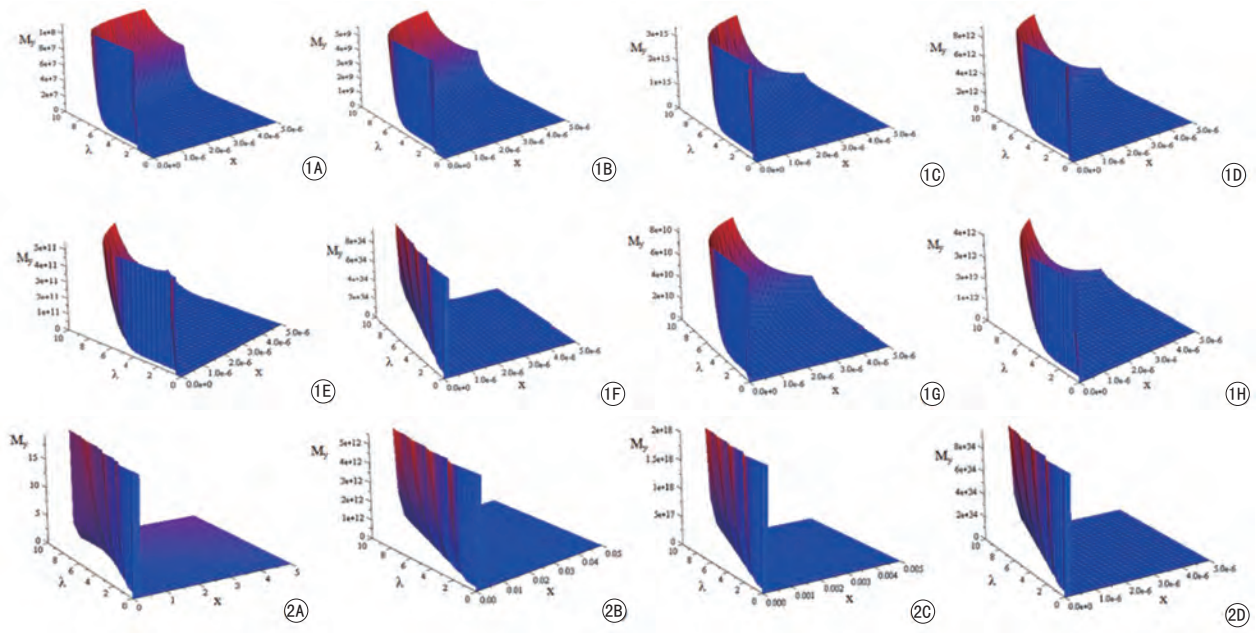

Fig. 1 The plots of transverse magnetization against x and λ [using equation (12)] for a time of 2 s, using the relaxation-time values at 1.5 T[23] of (A) skeletal muscle (B) heart muscle (C) liver (D) kidney (E) spleen (F) fatty tissue (G) gray brain matter (H) white brain matter. **Fig. 2** The plots of transverse magnetization against x and λ [using equation (12)] for a time of 2 s and the relaxation-time values at 1.5 T[23] of fatty tissue within the ranges (A) x: 0—5 m, (B) x: 0—0.05 m, (C) x: 0—0.005 m, (D) x: 0—0.000005 m.

In equations (26a, 27a and 27b), Γ (*m*+*f*+1) is the gamma function.

4 Conclusion

We have solved the time independent NMR flow equation and obtained analytical solutions for the NMR transverse magnetizations in terms of Bessel properties and functions which can reveal wealth of MRI physics and make NMR theory, dynamics and applications more interesting, appealing, motivating and exciting. It is significant to note from equations (8, 11) that the duration of time when the pulse is applied depends completely on the relaxation parameters of the sample. This makes the technique presented in this report uniquely applicable to anisotropic tissues. For illustration, from figures 1—3, the changes in the MRI experimental parameters $\lambda=\gamma G\delta$ and the signal are spatially represented at the microscopic level. It is observed that MRI signal decreases with increase in either T_1 or T_2 relaxation parameters. This can be very useful in planning for appropriate MRI experiments. Figure 3, is based on equations(10,12) which is completely described by the Bessel functions and properties in terms of MRI experimental parameters.

The behaviour of the transverse magnetizations and the MRI parameters are completely controlled by Bessel functions. This can be extremely useful for MRI simulations of Biological and Physiological systems.

Based on equations (3b, 5, 24, 25), quantity b depends on the NMR hardware especially the radiofrequency coil in use and the pulse program controlling it but does not depend on the diffusion constant. The computer program can be designed accordingly using the Bessel functions and properties. It is noteworthy that in the traditional NMR/MRI experiments, the expression for the b-value usually becomes more complicated if various NMR sequence intricacies are taken into account. Most importantly, it is assumed that the diffusion gradients are switched on for a negligible period of time in comparison with the diffusion time. However, Equation (24) does capture the most important features-square dependency on the gradient moment $G\delta$ and linear dependency on the diffusion time t.

The NMR signal from nuclei following the simple diffusion model is attenuated due to phase randomization as

$$\frac{S}{S_0} = \cos^n\left(\sqrt{\frac{2bD}{n}}\right) \tag{28}$$

This is a "discrete" form of the Stejskal-Tanner equation; equation (28) offers the possibility to measure the diffusion constant. This can be done by acquiring signals with and without diffusion gradients and calculating D. Better still, one can obtain the signal many times with different b-values and obtain D by a fitting procedure from equation (28). However, equation (4) can generate functions as solutions to various differential equations applicable in MRI physics, typically describing wavelike oscillatory behavior or a combination of oscillation and exponential decay or growth. For example, if q=2 in equation (3b) gives the phase of the spins as

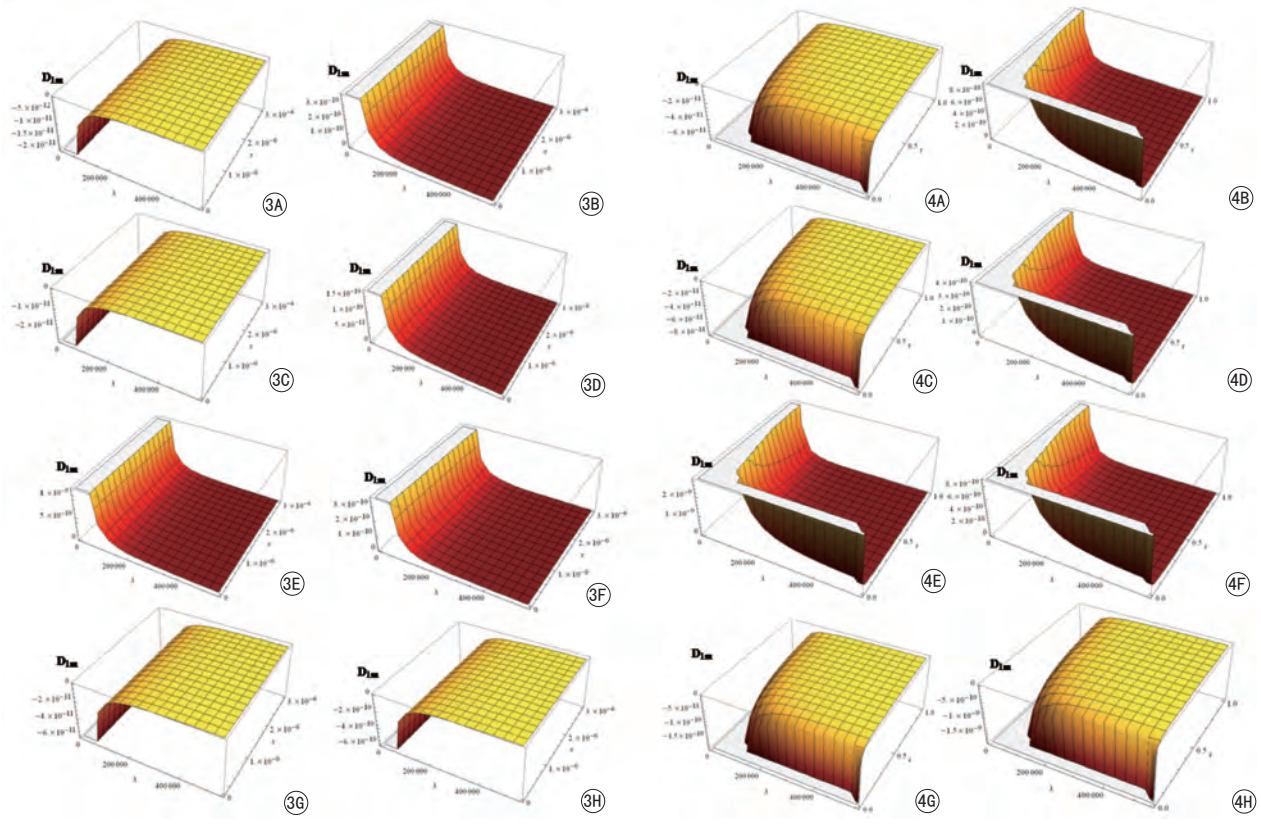

Fig. 3 Plots of D_{1m} against λ and x, for τ=1.0 s and the relaxation-time values at 1.5 T[23] of (A) skeletal muscle (B) heart muscle (C) liver (D) kidney (E) spleen (F) fatty tissue (G) gray brain matter (H) white brain matter. **Fig. 4** Plots of D_{1m} against λ and τ, for x=3 μm and the relaxation-time values at 1.5 T[23] of (A) skeletal muscle (B) heart muscle (C) liver (D) kidney (E) spleen (F) fatty tissue (G) gray brain matter (H) white brain matter.

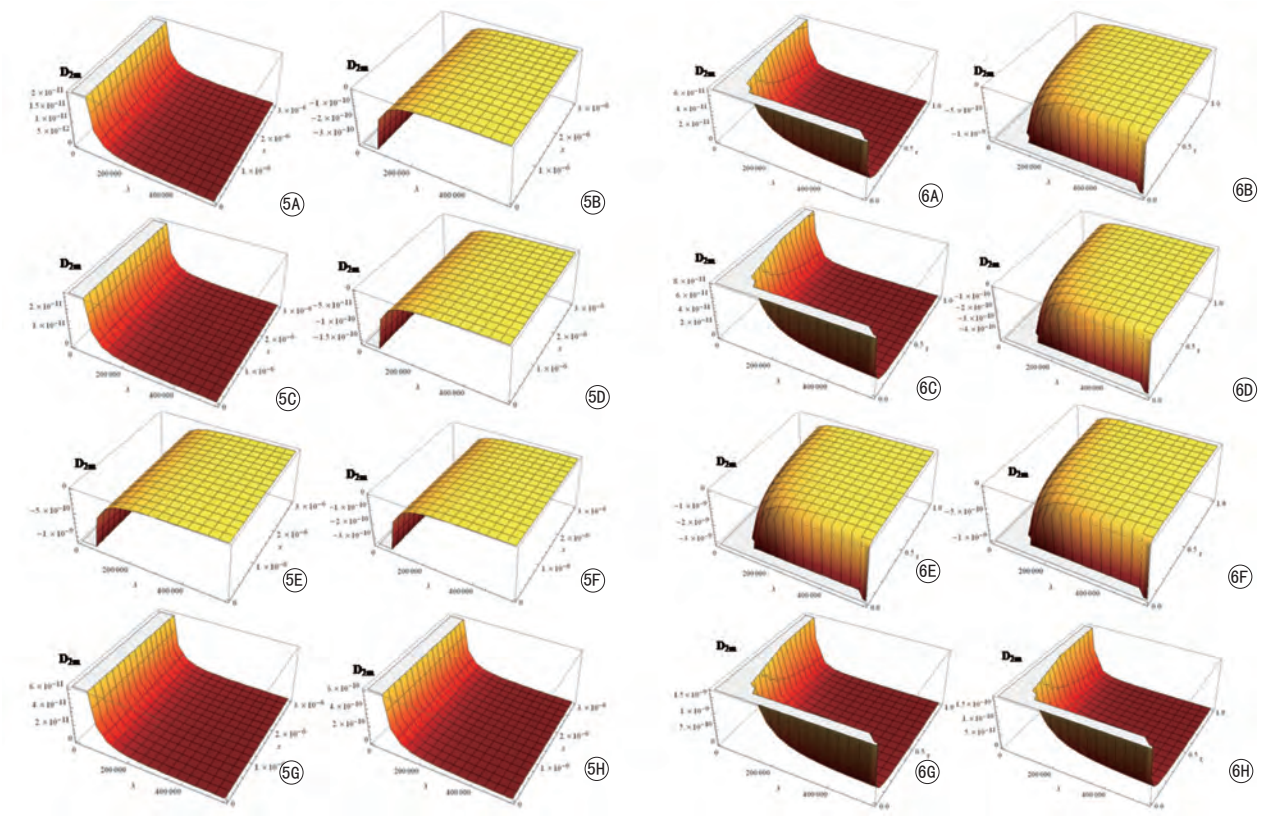

Fig. 5 Plots of D_{2m} against λ and x, for τ =1.0 s and the relaxation-time values at 1.5 T[23] of (A) skeletal muscle (B) heart muscle (C) liver (D) kidney (E) spleen (F) fatty tissue (G) gray brain matter (H) white brain matter. **Fig. 6** Plots of D_{2m} against λ and τ, for x=3 μm and the relaxation-time values at 1.5 T[23] of (A) skeletal muscle (B) heart muscle (C) liver (D) kidney (E) spleen (F) fatty tissue (G) gray brain matter (H) white brain matter.

$$\phi = \gamma G \delta x = \lambda x = \sqrt{\frac{2bD}{n}} \qquad (29a)$$

where the *b*–value is,

$$b=\gamma^2 G^2 \delta^2 \tau = \lambda^2 \tau \qquad (29b)$$

For the NMR transverse magnetization represented in figures 4—5, we can easily determine the value of D, G or τ based on equations (8, 9, 29) for anisotropic tissue environment where the value of T_1 and T_2 relxation parameters may vary acording to directional preference. In this way the diffusion coefficient is proportional to the characteristic angle of the transverse magnetization. Figure 6 shows that the field gradient G, depends completely on T_1 and T_2 relaxation parameters. Figure 7 gives unique contrasts for different human tissues at 1.5 T, and the images show the possibility of using Equations (26a and 26b) for spatial diffusion mapping. This may prove to be very useful in the study of tissue diseases in which diffusion properties are progressively affected.

It may be significant to note for example in edema with variable wall thickness, a solution for the rotation, moment and shear force on the cylinder requires successive differentiation of equation (17) starting from a knowledge of the deflection of the structure. The radial deflection of the cylinder can be shown to be:

$$M_y(x) = c_1(ber_m'(\lambda x) + ibei_m'(\lambda x)) + c_2(\ker_m'(\lambda x) + ikei_m'(\lambda x)) \qquad (30)$$

where *ber'*(λx), *bei'*(λx), *ker'*(λx) and *kei'*(λx) are the first derivatives of equation (17). The terms c_1 and c_2 are constants that are to bedetermined from the boundary conditions for the particular problem being investigated[24]. The derivative dM_y/dx gives the rotation of the cylinder. The bending moment is obtained from $\mu_x = -DdM_y^2/dx^2$ and the radial shear force $S_x = d\mu_x/dx$[24]. These parameters, with some modifications, can be used to obtain solutions for a range of medical and biomedical problems. In

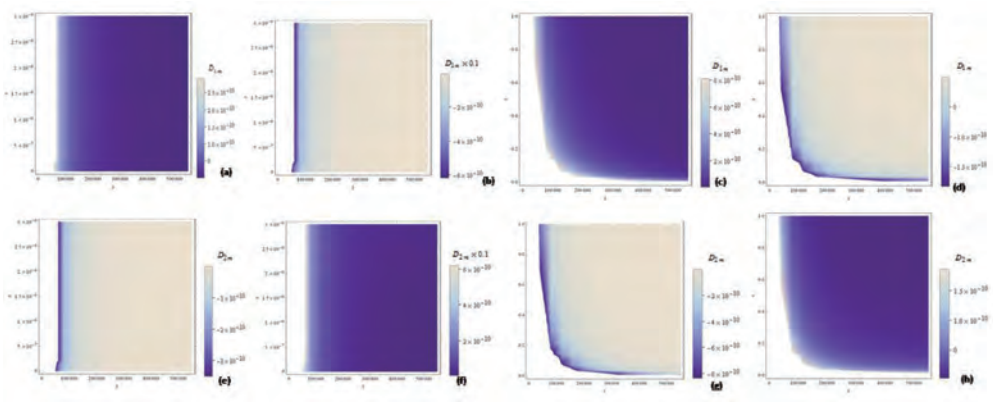

Fig. 7 Density plots of (A) D_{1m} against λ and x, τ=1.0 s for fatty tissue at 1.5 T[23] (B) D_{1m} against λ and x, τ=1.0 s for gray brain matter at 1.5 T (C) D1m against λ and τ, x=3 μm for fatty tissue at 1.5 T (D) D1m against λ and τ, x=3 μm for gray brain matter at 1.5 T (E) D_{2m} against λ and x, τ=1.0 s for fatty tissue at 1.5 T[23] (F) D_{2m} against λ and x, τ=1.0 s for gray brain matter at 1.5 T (G) D_{2m} against λ and τ, x=3 μm for fatty tissue at 1.5 T (H) D_{2m} against λ and τ, x=3 μm for gray brain matter at 1.5 T.

our next investigation, a mathematical model and computational analysis of nano drugs based on Bloch NMR flow equation and Bessel functions will be in focus where the properties of equation (4) will be explored to monitor the effects of drugs on the functional activities of different tissues especially the brain.

志谢 感谢中国科学院高能物理研究所单保慈教授翻译本文摘要

References

[1] Basser PJ, Mattiello J, LeBihan D. MR diffusion tensor spectroscopy and imaging. Biophys J, 1994, 66(1):259-267.

[2] Hahn E. Spin echoes. Phys Rev, 1950, 80:580-594.

[3] Carr E, Purcell E. Effects of diffusion on free precession in nuclear magnetic resonance experiments. Phys Rev, 1954, 94: 630-638.

[4] Torrey HC. Bloch equations with diffusion terms. Phys Rev, 1956, 104: 563-566.

[5] Stejskal EO, Tanner JE. Spin diffusion measurements: spin echoes in the presence of a time-dependent field gradient. J Chem Phys, 1965, 42:288-292.

[6] Tanner J, Stejskal E. Restricted self-diffusion of protons in colloidal systems by the pulsed-gradient, spin echo method. J Chem Phys, 1968, 49:1768-1777.

[7] Nicholson C, Phillips JM. Ion diffusion modified by tortuosity and volume fraction in the extracellular microenvironment of the rat cerebellum. J Physiol, 1981, 321:225-257.

[8] Hrabe J, Hrabetova S, Segeth K. A model of effective diffusion and tortuosity in the extracellular space of the brain. Biophys J, 2004, 87(3):1606-1617.

[9] Kingsley PB. Introduction to diffusion tensor imaging mathematics: Part I. Tensors, rotations and eigenvectors. Part A. Concepts Magn Reson, 2006, 28:101-122.

[10] Kingsley PB. Introduction to diffusion tensor imaging mathematics: Part II. Anisotropy, diffusion-weighting factors and gradient encoding schemes. Part A. Concepts Magn Reson, 2006, 28A: 123-154.

[11] Kingsley PB. Introduction to diffusion tensor imaging mathematics: Part III. Tensor calculation, noise, simulations and optimization.. Part A. Concepts Magn Reson, 2006, 28A: 155-179.

[12] Lim KO, Helpern JA. Neuropsychiatric applications of DTI-a review. NMR Biomed, 2002, 15(7-8): 587-593.

[13] Callaghan PT. Principles of nuclear magnetic resonance microscopy. New York: Oxford University Press, 1991.

[14] Haacke ME, Brown RW, Thompson MR, et al. Magnetic resonance imaging: physical principles and sequence design. New York: John Wiley and Sons, 1999.

[15] Chandrasekhar S. Stochastic problems in physics and astronomy. Rev Modern Physics, 1943, 15:1-89.

[16] Awojoyogbe OB, Dada OM, Faromika OP, et al. Mathematical concept of the bloch flow equations for general magnetic resonance imaging: a review. Concepts in Magnetic Resonance Part A, 2011, 38A (3): 85-101.

[17] Dada M, Faromika OP, Awojoyogbe OB, et al. The impact of geometry factors on NMR diffusion measurements by the stejskal and tanner pulsed gradients method. Int J Theoretical Physics, 2011, 15: 1-2.

[18] Awojoyogbe OB. Analytical solution of the time dependent bloch NMR equations: a translational mechanical approach. Physica A, 2004, 339: 437-460.

[19] Awojoyogbe OB. A mathematical model of bloch NMR equations for quantitative analysis of blood flow in blood vessels with changing cross-section II. Physica A, 2003, 323c: 534-550.

[20] Awojoyogbe OB. A mathematical model of bloch NMR equations for quantitative analysis of blood flow in blood vessels with changing cross-section I. Physica A, 2002, 303: 163-175.

[21] Awojoyogbe OB. A quantum mechanical model of the bloch NMR flow equations for electron dynamics in fluids at the molecular level. Phys Scr, 2007, 75: 788-794.

[22] Awojoyogbe OB, Boubaker K. A solution to bloch NMR flow equations for the analysis of hemodynamic functions of blood flow system using m-Boubaker polynomials. Int J Current Applied Phy, 2009, 9 (1): 278-283.

[23] Bottomley PA, Foster TH, Argersinger RE, et al. A review of normal tissue NMR relaxation times and relaxation mechanisms from 1 to 100 MHz: dependence on tissue type, NMR frequency, temperature, species, excision, and age. Med Phys, 1984, 11(4): 425-448.

[24] Andrew C. Whyte. Kelvin functions and their derivatives. Available at: http//www.acwhyte. fsnet.co.uk

[25] Abramowitz M, Stegun IA. Handbook of Mathematical Functions with Formulas, Graphs, and Mathematical Tables. 9th. New York: Dover, 1972: 379-381.

[26] Prudnikov AP, Marichev OI, Brychkov YA. The Kelvin Functions bernu(x) , beinu(x), ker_nu(x) and keinu(x). Newark NJ: Gordon and Breach, 1990: 29-30.

[27] Spanier J, Oldham KB. The Kelvin Functions. Washington: Hemisphere, 1987: 543-554.